

Highly accurate O(N) method for delocalized systems

Yuriko Aoki · Oleksandr Loboda · Kai Liu ·
Marcin A. Makowski · Feng Long Gu

Received: 28 December 2010 / Accepted: 27 July 2011 / Published online: 10 September 2011
© Springer-Verlag 2011

Abstract The elongation method, developed in our groups, is an ab initio method approaching order O(N) type scalability with high efficiency and high accuracy (error $<10^{-8}$ au/atom in total energy compared to the conventional calculation) that can be applied to any one-dimensional (polymer), two-dimensional (surface) or three-dimensional (solid material) systems. For strongly

delocalized systems, however, the accuracy of the original elongation method for the targeted entire systems declines by approximately two orders of magnitude in the total energy as compared to the value obtained by the earlier implemented version of the elongation method for nondelocalized systems. The relatively small differences (10^{-6} – 10^{-8} au) between the elongation method and conventional method total energies have caused more serious errors in the second hyperpolarizability, γ , especially in nano-scale systems which have accompanying strong delocalization. In order to solve this problem, we have incorporated a simple correction technique based on an additional “orbital basis” to the “region basis” in our original elongation method procedures. Some not so-well-localized orbitals are incorporated into the interaction with the attacking molecule. This treatment has been applied to some model nano- and bio-systems that previously have shown strong delocalization, and the high accuracy in the energy obtained for nonstrongly delocalized systems was retained even for the strongly delocalized systems, both for the energies and for the second hyperpolarizabilities. This is a major breakthrough and now expands the systems for which the elongation method can be used to calculate and predict second-order nonlinear optical properties for delocalized systems.

Dedicated to Professor Akira Imamura on the occasion of his 77th birthday and published as part of the Imamura Festschrift Issue.

Y. Aoki (✉) · O. Loboda · M. A. Makowski
Department of Material Sciences, Faculty of Engineering
Sciences, Kyushu University, 6-1 Kasuga-Park,
Fukuoka 816-8580, Japan
e-mail: aoki@mm.kyushu-u.ac.jp
URL: http://aoki.cube.kyushu-u.ac.jp/index_top-e.html

O. Loboda
e-mail: loboda@mm.kyushu-u.ac.jp; oleksandras@gmail.com

M. A. Makowski
e-mail: makowskm@chemia.uj.edu.pl

Y. Aoki · F. L. Gu
Japan Science and Technology Agency, CREST,
4-1-8 Hon-chou, Kawaguchi, Saitama 332-0012, Japan

K. Liu
Department of Molecular and Material Sciences,
Interdisciplinary Graduate School of Engineering Sciences,
Kyushu University, 6-1 Kasuga-Park, Fukuoka 816-8580, Japan
e-mail: ak-l-kai@mms.kyushu-u.ac.jp

M. A. Makowski
Department of Theoretical Chemistry, Jagiellonian University,
Ingardena 3, 30-060 Krakow, Poland

F. L. Gu (✉)
Center for Computational Quantum Chemistry, South China
Normal University, Guangzhou 510631, China
e-mail: gu@scnu.edu.cn

Keywords Elongation method · Ab initio method ·
Nanotube · Lycopene · β -carotene · Fullerene ·
Porphyrin · Nanowire

Abbreviations

RLMO	Region localized molecular orbital
QFMM	Quantum fast multipole method
SW-BN/CNT	Single-wall boron nitride/carbon nanotube
SW-BNNT	Single-wall boron nitride nanotubes

OTE	Oligo(2,5-thienylene-ethynylene)
H ₂ TPP	Free base tetraphenylporphyrin
NLO	Nonlinear optics
CMO	Canonical molecular orbital

1 Introduction

In 1991, the elongation method, an efficient method for quantum mechanical calculations of large systems, was originally proposed by Imamura [1] during one of his stays in Heidelberg, Germany. To commemorate the 77th birthday of Professor Akira Imamura, his many accomplishments in theoretical chemistry and physics, including the development of many semi-empirical and *ab initio* methods, the Editor in Chief of TCA, Prof. Chris Cramer has allowed myself and Prof. K. J. Jalkanen to be guest editors for this special Festschrift issue of TCA. Although in the early 1990s the concept of and need for order- N [O(N)] methods didn't exist, Prof. Akira Imamura was thinking about "how to avoid direct SCF calculations for large biological systems (biopolymers composed of hundreds if not thousands of residues of amino acids or nucleic acid base pairs in proteins and DNA or RNA) by treating only the local interactions between a few neighbor residues in large systems". While contemplating how to perform such calculations, he got the idea of theoretically simulating the synthesis of polymers so as to mimic the chemical reactions that occur in nature during polymerization reactions to form peptides, proteins and polynucleotides. Hence he named the method he developed the elongation method, due to the nature of the first so-called buildup of the model from calculations for monomeric units. By doing so, he developed one of the first O(N) methods. First, he developed the method conceptually and then he coded it at the extended Hückel level [1] and was then able to confirm that it was working well and achieved very good accuracy in comparison with the more expensive conventional methods. Subsequently, in his group at Hiroshima University, we have continued to develop and extend this method at the *ab initio* single determinant Hartree–Fock level of theory [2], at the Kohn–Sham density functional theory (KS-DFT) level of theory [3], and subsequently, in my group at Kyushu University, including electron correlation effects at the *ab initio* wave function theory (WFT) at the Møller–Plesset perturbation theory to second-order (MP2) [4]. This is line with the early work by Professor Imamura on the development of rules for chemical reactions for both ground and excited electronic state chemical reactions, the so-called Woodward–Hoffmann rules, which are necessary to understand in order to gain a better understanding of physical and chemical properties of large biological

systems. For a good review of the various extensions to the original elongation method which have been developed up until 2006, see Ref. [5].

Recent progress in developing linear scaling electronic structure methods has lead to the development of a variety of O(N) techniques [6, 7]. The Fermi operator expansion/projection (FOP/FOE) [8, 9], Density-Matrix Minimization methods [10] speak for themselves. The basic idea of Divide-and-Conquer [11] method is to calculate certain regions of the density matrix by considering sub-volumes and then to generate the full density matrix by adding these parts with the appropriate weights. The Orbital Minimization method [12] unlike Density-Matrix Minimization does not calculate the density matrix directly, but expresses it via Wannier functions. In the Optimal Basis Density-Matrix Minimization method [13], the fundamental basis functions are contracted in a first turn, then the Hamiltonian and overlap matrix are constructed in this new smaller basis. Many molecular properties remain for which to date no linear-scaling methods have been devised and implemented. The results for some molecular properties or electron correlation methods depend strongly on the size of the basis set. For example, post-Hartree–Fock methods require larger basis sets. This requirement rules out, in particular, the Density-Matrix Minimization method which becomes inefficient if the number of basis functions per atom is very large. In this respect, it should be noted that even if a method scales linearly with molecular size, the computational cost may increase dramatically with the basis set size. Therefore, reducing the prefactors remains an important issue. The above-mentioned Orbital Minimization (OM) and Optimal Basis Density-Matrix Minimization methods suffer from ill-conditioning problems and therefore require frequently an excessive number of iterations, while in both OM and FOP methods, the pre-knowledge about the bonding properties is needed to form the initial guess [6]. Finally most of the linear scaling methods are known to fail when applied to metallic systems. Still, in spite of the fact that the various linear scaling methods and algorithms have been developed and applied in a large variety of fields, however, very little is known on the performance of such approaches for the computation of the NLO properties. Apart from the above-mentioned techniques, a branch of methods that explicitly divide molecular systems into smaller fragments has been proposed, from which divide and conquer [14–17], fragment molecular orbital [18–25], and density matrix renormalization group methods [26–28] are probably the most well known at the *ab initio* HF level of theory and are most actively being developed.

Our treatment is different from other linear scaling methods in adopting the concept of the Region Localized Molecular Orbitals (RLMOs) [29], and it has recently been

extended to be applicable for three-dimensional (3D) systems [30]. As an approach toward post-Hartree–Fock, we developed the elongation local MP2 (ELG-LMP2) method [4]. We also confirmed that the RLMO is very useful to evaluate local excitation around chromophore center in a large system at single excitation configuration interaction (CIS) and TDHF levels [31]. Furthermore, a so-called cut-off technique for the elongation method makes possible to deal with huge number of 2e-integrals of gigantic systems [32]. Additionally, Quantum Fast Multipole Method (QFMM) was incorporated into the elongation method at the Hartree–Fock and Density Functional Theory (DFT) levels [33–35].

In last decade, the elongation finite-field (elongation-FF) method has been developed in our laboratory [36]. In this approach, molecular (hyper)polarizabilities are obtained by numerically differentiating the total energy with respect to electric fields. This method has been applied to many quasi-one-dimensional π -electron conjugated organic polymers, such as polyacetylene, polydiacetylene, polythiophene, and their derivatives at both levels of semi-empirical and *ab initio* method [37–42]. Also recently it has been applied to gigantic systems as BNC nanotubes [40] and a porphyrine wire [41]. However, we found the fact that the fourth-order energy derivatives with respect to electric field sometimes cause a big error around 10–20% of conventional values especially in second hyperpolarizability (γ) even with 10^{-6} au/atom difference in the total energy between those by conventional method and elongation method.

The purpose of this work is to improve the accuracy of our elongation method to evaluate nonlinear optics (NLO) properties of polymers and to develop this method so as to be able to analyze the relationship between structure and NLO properties. Therefore, more accurate total energy evaluations with total energy error less than 10^{-10} au/atom are strongly desired to get acceptable hyper-polarizability values. For this purpose, we have extended the traditional elongation method that allows one to get very accurate total energies, so that one can get highly accurate higher order derivatives of the total energy efficiently. By this technique, the physical properties for strongly delocalized systems like carbon nanotubes and photonic polymers can be obtained under various applied external fields. The calculation of the NLO of such systems will play an important role in the next generation information and computing industry that will require device designs at the nano-level. In this paper, we show how total energies have been improved by our new development and present some preliminary NLO property results. This method development is essential for the elongation method and its applications to be able to treat bio-/nano-systems with orbital delocalization and its functional designing with high

accuracy. This method makes it possible to treat huge strongly delocalized systems that are formidable by the conventional method. In this paper, we focus not only on the total energy improvement but also on NLO property calculations. We have already reported computational time of our elongation method in other articles (see, for example, [4, 31–35, 40]).

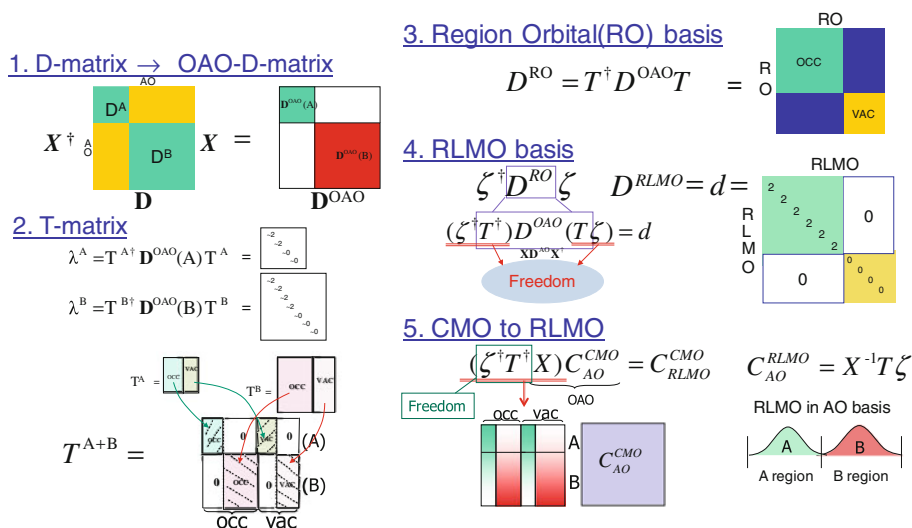
2 Outline of elongation method

The elongation method has been implemented in the GAMESS program package [43]. In the elongation procedure, the delocalized canonical molecular orbitals (CMOs) of a starting cluster are first localized into frozen and active regions in the specified parts of the molecule. The “specified parts” means appropriate size of A region and B region to get good localization as well as high accuracy for total energies (error of less than 10^{-8} au/atom) in comparison with that obtained by conventional methods. For getting this criterion, we normally select one unit as the A region and 3–5 units as the B region on which active RLMOs will be formed for the interaction with attacking monomer. Next, a monomer is attacking to the active region of the cluster, and the eigenvalue problem is solved by disregarding the localized molecular orbitals (LMOs) which have no or very weak interaction with the attacking monomer. By repeating this procedure, the length of the polymer chain is increased step by step to any desired length. The obvious advantage of the approach lies in the fact that one can avoid solving very large secular equations for large aperiodic systems.

Since the detailed explanation in making region LMO (RLMOs) in an efficient manner has been described in other articles by Gu et al. [29], here only the essential points of this method are explained with the illustrations as shown in Fig. 1. One can partition the starting cluster into two regions, region A (frozen region) and region B (active region), and localize the CMOs into these two regions. Region B is the one with atoms adjacent to the interactive end of the cluster, whereas region A is at the opposite end far away from the interactive center. It should be mentioned here that by using the density matrix, the partition of the starting cluster into two regions is unique since the AOs belonging either to A or B region are well defined. This is different from the other localization schemes, where the partitions are not unique. As one has already seen the division of CMOs into two regions is not so straightforward and poor selection leads to poor localization. The desired RLMOs can be obtained according to five steps as shown below and in Fig. 1.

1. As shown in Fig. 1 (step1), the density matrix in the orthogonal atomic orbital (OAO) basis is transferred

Fig. 1 Schematic illustration to show how to make RLMOs



from AO basis by X , where the following idempotence relation of the density matrix in an OAO basis

$$D^{\text{OAO}} D^{\text{OAO}} = 2D^{\text{OAO}} \quad (1)$$

is proved and the eigenvalues of D^{OAO} must be either 2 or 0. Therefore, the eigenvectors of D^{OAO} are well separated into occupied or vacant subspaces.

2. A regional orbital (RO) space is constructed by separately diagonalizing the $D^{\text{OAO}}(A)$ and $D^{\text{OAO}}(B)$, where $D^{\text{OAO}}(A)$ and $D^{\text{OAO}}(B)$ are the sub-blocks of D^{OAO} with AOs belonging to A and B regions, respectively. These eigenvectors span the RO space. The transformation from OAOs to ROs is given by the direct sum of T^A and T^B , where T^A and T^B are the eigenvectors of $D^{\text{OAO}}(A)$ and $D^{\text{OAO}}(B)$, respectively. Fig. 1 (step 2) shows the diagonalization of the matrices of $D^{\text{OAO}}(A)$ and $D^{\text{OAO}}(B)$ and the schematic construction of the T matrix. The corresponding eigenvalues are divided into three sets corresponding to ROs that are approximately doubly occupied (the value is close to 2), singly occupied (close to 1) and empty (close to 0). The singly occupied orbitals in A and B can be used to construct hybrid orbitals to form covalent bonding/antibonding pairs. For a nonbonded system, such as water chain, there are only two sets, either doubly occupied or empty. Fig. 1 (step 2) shows the latter case.

3. The RO density matrix is obtained by transforming the D^{OAO} by T matrix combined by T^A and T^B as shown in Fig. 1 (step 3). Using Eq. 1 and the unitary condition $TT^\dagger = T^\dagger T = 1$, one can verify that

$$D^{\text{RO}} D^{\text{RO}} = 2D^{\text{RO}}. \quad (2)$$

4. Except for orthogonalization tails the ROs given above are completely localized to region A or region B.

However, they are not completely occupied or unoccupied. Thus, final step is to carry out a unitary transformation between the occupied and unoccupied blocks of D^{RO} to keep the localization as large as possible. Then the only nonzero elements of D^{RLMO} are equal to 2 (cf. Eq. 2). As shown in the Fig. 1 (step 4) when D^{RO} is transferred back into D^{OAO} , one can see that $T\zeta$ gives the transformation matrix of D^{OAO} . The $T\zeta$ values have plenty of freedom in the framework of a unitary transformation because the eigenvalues of D^{OAO} are degenerate by 2 in occupied space and by 0 in unoccupied space. Nevertheless, we can define the transformation matrix, $T\zeta$, so that the RLMOs are localized to the largest extent possible into A(frozen) or B(active) regions “through T matrix”, because we can get the RLMO coefficients similar to the T matrix in this special localization scheme. Thus, finally obtained $T\zeta$ becomes very similar to the original T matrix in OAO basis.

5. Finally, the unitary transformation from CMO to RLMO is given in the Fig. 1 (step 5). After transferring $T\zeta$ back to the AO basis by using X , we can get the RLMO coefficients in the AO basis as shown in the right hand side of the Fig. 1 (step 5).

After the well-localized RLMOs are obtained by the above procedure, the Fock matrix based on the RLMOs is expressed only by using active RLMOs as shown in Fig. 2, in which frozen RLMOs are removed before interaction with the attacking monomer. Then our working space is defined by the RLMOs assigned to the B region together with the CMOs of the attacking monomer. For a given suitably large starting cluster, the interaction between the frozen region and the attacking monomer is minimized by using RLMOs. In our treatment, the proper size of the

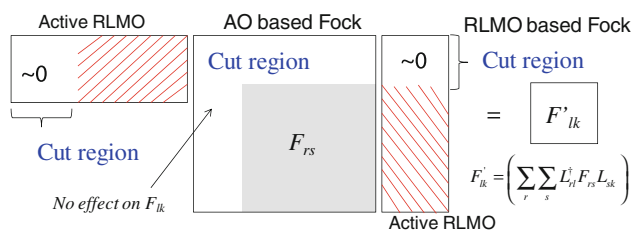


Fig. 2 Schematic illustration to make RLMO based Fock matrix

starting cluster is automatically detected during elongation from a rather small starting cluster and the elongation process with a reduced number of RLMOs is initiated after the condition to remove the frozen orbitals is satisfied. The elongation Hartree–Fock equation is solved self-consistently in the localized orbital space of the interactive region, or more precisely, the working space consists of RLMOs of the active region and CMOs of the attacking monomer. This solution yields a set of CMOs in the reduced space which can be localized again into a new frozen region and a new active region. The whole procedure is repeated until the desired length is reached. The important feature of the elongation method is that the Hartree–Fock equation is solved only for the interactive region instead of the whole system. As the system enlarges, the size of the interactive region is almost the same as that of the starting cluster and the CPU required in the elongation SCF is more or less constant. Additionally, the “Cut region” in the AO based Fock matrix of Fig. 2, the region far from the attacking monomer, has no contribution on the final RLMO-based Fock matrix because the corresponding coefficients part of the active RLMOs should be almost zero as written by “ ~ 0 ” in the active RLMO coefficients. So we can get rid of not only the frozen RLMOs, but also the frozen part in the AO-based Fock matrix elements, leading to big reduction in making Fock matrix and $O(N)$ computational time during the elongation process. The details about cutoff procedure are described in our recent papers [32, 35].

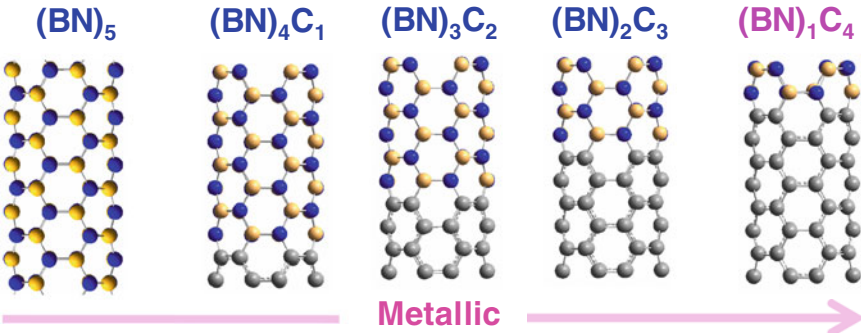
3 Problem in old elongation method

Although we can elongate both periodic and aperiodic one-dimensional systems, some problems remain in strongly delocalized systems. For example, if the system has strongly delocalized π orbitals, our treatment does not provide satisfied accuracy in the total energies in comparison with conventional direct calculations. This causes sometimes a big error especially in the second hyperpolarizability (γ) which is given by fourth-order energy derivatives. However, significantly large hyperpolarizability is mostly found in strongly delocalized large systems,

and thus, a highly accurate computational method for such systems is desired to design useful NLO materials.

The example which shows the difficulty to calculate accurate energies for delocalized systems with the traditional elongation method is given by the carbon-rich single-wall boron nitride/carbon nanotube (SW-BN/CNT) as shown in Table 1. It is reported that the electronic band gap of single-wall boron nitride nanotubes (SW-BNNTs) can be reduced by adding C atoms into the structure [44, 45], and so carbon-rich BN/CNT that possesses delocalized π -electrons can be a good model to examine the applicability of our new treatment. Calculations of the electronic structures were performed for pristine SW-BNNTs with different diameters and chirality. We confirmed that the accuracy depends on the size of the diameter rather than on the basis set. The errors in total energy become larger with increasing diameter size, because π -electron delocalization effects become stronger in larger diameter nanotubes [40]. Then we focus on (4, 4) BN/C heterostructured nanotubes [(BN) $_x$ C $_y$ ($x, y = 1-4, x + y = 5$)] including carbon atoms that make the delocalization stronger with included C ratio in the framework of HF/STO-3G theory. The periodic structures are optimized by using the Gaussian 03 program [46] at the B3LYP/6-31G level. The total energy difference between elongation method and conventional direct method is listed in Table 1, where some of the data for different sizes are from the Ref. [40]. The N_{st} in the table means the starting cluster size in our elongation method. In Table 1, the number of units 6 and 7 (112 and 128 atoms, respectively) corresponds to the number of units in the starting cluster and in the first elongation step for $N_{st} = 6$, respectively, while the Number of units 10 and 11 (176 and 192 atoms, respectively) corresponds to the number of units in the starting cluster and in the first elongation step for $N_{st} = 10$, respectively. This information is important to see how large errors are induced by one elongation step. In addition, the information concerning the last step, with the number of units 20 (336 atoms), is also important. We also show the results obtained during the elongation procedure for 11 units and 17 units as examples. The results obtained for 6–20 units have already been reported in Table 6 of Ref. [40], and here we just present a small cross section of that data to document the results. When $N_{st} = 6$, it can be seen that the errors per atom for four systems are very small, but increase with the carbon content because of more delocalization in carbon’s nature; especially for carbon rich system, (BN) $_1$ C $_4$, the error $\sim 10^{-6}$ au/atom is not acceptable to calculate reliable γ as seen from the example of metalloporphyrin arrays. So, for (BN) $_1$ C $_4$ and (BN) $_2$ C $_3$, we recalculated their energies by using the larger-sized starting cluster $N_{st} = 10$. As a result, the error per atom is decreased to 10^{-8} au for $N_{st} = 10$, but β and γ values still show unstable curves as a function of

Table 1 Structure of the (4, 4) pristine and BN/C heterostructured nanotubes $(\text{BN})_x\text{C}_y$ ($x, y = 1-4$, $x + y = 5$). The elongation errors (au/atom) in total energy are shown for different starting cluster size (N_{st})



Number of units	Number of atoms	$N_{\text{st}}=6$ (Starting cluster size)				$N_{\text{st}}=10$	
		$(\text{BN})_4\text{C}_1$	$(\text{BN})_3\text{C}_2$	$(\text{BN})_2\text{C}_3$	$(\text{BN})_1\text{C}_4$	$(\text{BN})_2\text{C}_3$	$(\text{BN})_1\text{C}_4$
6	112	0.000E+00	0.000E+00	0.000E+00	0.000E+00		
7	128	7.945E-10	3.680E-09	2.336E-08	3.059E-07		
10	176	7.379E-09	4.901E-08	5.006E-07	6.209E-06	0.000E+00	0.000E+00
11	192	7.748E-09	3.927E-08	4.255E-07	5.137E-06	3.167E-10	9.695E-09
17	288	1.144E-08	5.598E-08	5.851E-07	7.054E-06	1.872E-09	2.881E-08
20	336	1.505E-08	7.742E-08	7.713E-07	9.186E-06	5.283E-09	3.829E-08

the number of units as seen in Fig. 3 of Ref. [40]. We have already confirmed that the delocalized π -orbitals from carbon atoms give small band gaps, which cause insufficient accuracy in the total energy calculations during elongation process which is required for the calculation of nonlinear optical properties, for example, second (hyper)polarizabilities.

To solve the problem of insufficient accuracy and inefficiency in delocalized systems, we propose here a simple technique to incorporate the delocalized frozen orbitals into the active space, and the results tested for some nano- and bio-systems using this treatment are shown in the next section.

4 How to treat delocalized orbitals

The problem in the accuracy is caused by the fact that we only treated the RLMOs as the “region” basis when we judge if we discard the frozen RLMOs that located farthest from attacking monomer or not. That is, when the contribution from active RLMOs on the frozen terminal unit

$$P(A_1) = \sum_r^{\text{on}A_1} \sum_s^{\text{on}A_1} C_{ri}^{\text{Active RLMO}} S_{rs} C_{si}^{\text{Active RLMO}} \quad (3)$$

is less than the threshold value (for example, 10^{-5}), we can start the elongation and then we can disregard all the frozen RLMOs on the frozen terminal unit. The active RLMOs are already sufficiently included in the interaction with

attacking monomer under the defined threshold. If the threshold value, $P(A_1)$, is set tight, the elongation starts late after several elongation steps, and then the number of active RLMOs to be included into active space increases, leading more accurate results with longer CPU time. On the other hand, the threshold value is set too loose, the elongation starts early, and then the number of active RLMOs decreases, leading to less accurate results with shorter CPU time. For delocalized systems, however, the elongation process sometimes even does not start unless we set the threshold very loose because some orbitals that cannot inherently be localized still remain on the frozen region. This fact forces the threshold very loose to start elongation process for delocalized systems, and thus the obtained accuracy becomes worse compared to that for other systems. We call it as “region basis concept” because a set of the frozen orbitals in the frozen region has two choices of either being included into active region or discarded. However, the number of delocalized RLMOs (almost similar shape to CMOs) is limited to a few frozen orbitals and kept almost constant during the elongation process. So, CPU time consumed for this inclusion may not be accumulated during the process. To improve the accuracy in “region basis concept” mentioned above, we introduce “orbital basis concept” together with the “region basis concept” for the more effective selection of necessary active orbitals.

For any RLMO of the starting cluster, one can initially define the overlap between pair of frozen RLMO and active RLMO as,

$$Q_{ij} = \left\langle \phi_i^{\text{Frozen RLMO}}(\text{A}) \left| \phi_j^{\text{Active RLMO}}(\text{B}) \right. \right\rangle. \quad (4)$$

With this quantity, we can find the i -th frozen RLMOs that are associated with j -th active RLMOs with an overlap larger than the threshold value (we set 10^{-4} as the default). If some frozen RLMOs have values of Q_{ij} larger than the threshold, these orbitals are still assigned to the delocalized group even after the localization process and are transferred back into active RLMO group to join the interaction with the attacking monomer. Only the remaining frozen RLMOs are assigned to “truly frozen” orbitals that never interact with the attacking monomer hereafter. In the next elongation step, we also check the Q_{ij} value again in the next boundary between frozen region and active regions, and then detected delocalized orbitals are always transferred back into active RLMO group. By continuing this treatment through all the elongation steps, delocalized orbitals are always picked up and shifted to active space to give a more correct result. In addition, the number of shifted orbitals is not increased at the next elongation step because the number of targeted orbitals on the boundary between frozen and active regions remains always essentially the same. As a result, the computational time is not accumulated and even become shorter since this treatment makes the elongation start earlier from small starting cluster with keeping the accuracy high. Finally, we get excellent agreement with the total energy calculated by conventional method even for strongly delocalized systems. The schematic illustration of delocalized orbitals is drawn in Fig. 3 as a model of SW BN/CNT. It can be seen from the figure that the blue orbitals originally assigned as frozen RLMOs have some overlap with pink active RLMOs over the A and B regions as far as the tailing of frozen RLMOs is permeated into B region. These orbitals correspond to those we should still include into the

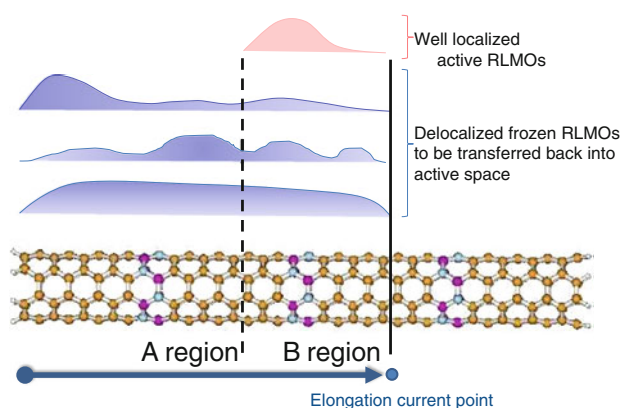


Fig. 3 Schematic illustration of the shape of well localized (ideal) active RLMOs and delocalized frozen RLMOs to be shifted to active RLMO group

active RLMO group toward the interaction with attacking monomer.

5 Results for selected systems

5.1 SW-BN/CNT

The treatment described in the previous section was applied first to the carbon-rich (4,4) SW-BN/CNT, $(\text{BN})_1\text{C}_4$, system that provided worse results in accuracy compared to $(\text{BN})_5$, $(\text{BN})_4\text{C}_1$, $(\text{BN})_3\text{C}_2$, and $(\text{BN})_2\text{C}_3$ as shown in Table 1. The resultant errors by the revised elongation method, denoted by New_Elg, are listed in Table 2 in comparison with those by traditional elongation method, denoted by Old_Elg. The table shows that the accuracy was around two orders of magnitude improved by the revised elongation method. These results are promising to get reliable results when we apply it to more delocalized systems not only in conjugated hydrocarbon systems but also metallic systems.

5.2 Polyacene

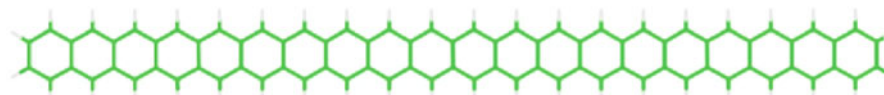
Another delocalized example, polyacene, as shown in Table 3, is tested by using both old and new elongation methods as a first step to apply our method to the most intractable two dimensional graphene sheet. This system possesses even more delocalized π -orbitals than SW-BN/CNT because all of them locate completely perpendicular to the plane. This fact can be suggested also from larger errors in SW-BN/CNT system with larger diameter [40]. With the old elongation method, the accuracy depends on the basis set size because larger basis set makes the localization worse, leading to larger errors in total energy. However, one can see that the errors by STO-3G basis set are improved only by one-order of magnitude in the new

Table 2 Error per atom (in au) introduced by the old and new elongation methods for (4,4)SW-BN/CNT, $(\text{BN})_1\text{C}_4$, at the HF/STO-3G level

Atoms	Total energy Conv (in au)	Old_Elg Error/atom	New_Elg Error/atom
112	-3654.67279190	0.00E+00	0.00E+00
128	-4253.10068386	3.06E-07	1.68E-09
144	-4851.70684615	2.97E-06	8.93E-09
160	-5450.18308411	4.60E-06	3.66E-08
176	-6048.76373323	6.21E-06	1.75E-08
192	-6674.65602795	5.14E-06	1.50E-08
208	-7273.24074195	5.71E-06	1.70E-08

(BN)₁C₄
Periodic unit

Table 3 Error per atom (in au) introduced by the old and new elongation methods for polyacene chain at the HF/STO-3G and 6-31G(d) level



Step	Number of units (rings)	Number of atoms	Old_Elg	New_Elg	Old_Elg	New_Elg
			Error/atom	Error/atom	Error/atom	Error/atom
			STO-3G		6-31G(d)	
0	6	42	0.00E+00	0.00E+00	0.00E+00	0.00E+00
1	7	48	1.51E-05	2.51E-07	1.03E-04	2.06E-07
2	8	54	2.97E-05	5.64E-07	1.64E-04	5.13E-07
3	9	60	4.24E-05	8.61E-07	2.42E-04	8.52E-07
4	10	66	5.31E-05	1.12E-06	2.83E-04	1.17E-06
5	11	72	6.21E-05	1.34E-06	3.17E-04	1.46E-06
6	12	78	6.98E-05	1.53E-06	3.46E-04	1.73E-06
7	13	84	7.63E-05	1.69E-06	3.71E-04	1.96E-06
8	14	90	8.20E-05	1.83E-06	3.93E-04	2.17E-06
9	15	96	8.70E-05	1.95E-06	4.12E-04	2.35E-06
10	16	102	9.14E-05	2.06E-06	4.28E-04	2.53E-06
11	17	108	9.53E-05	2.15E-06	4.58E-04	2.68E-06
12	18	114	9.87E-05	2.24E-06	4.84E-04	2.84E-06
13	20	126	1.01E-04	2.32E-06	4.77E-04	3.00E-06

method while those by 6-31G(d) are by two-orders of magnitude. This fact suggests that this correction technique provides always good results even for strongly π -electron delocalized systems almost regardless of the basis set size. If the more tight threshold for Q_{ij} is used, the more accurate results must be expected because a few more frozen orbitals accompanied by small overlap with active RLMOs are additionally joined to the interaction with attacking monomer. If an infinite zero threshold is used, all the orbitals are admitted to the SCF calculations and then obtained results are completely same as those by the conventional method though this situation is meaningless.

5.3 β -carotene

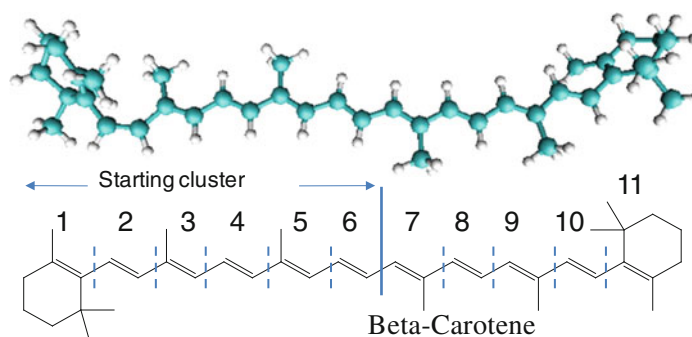
As an application to bio-system, we applied our treatment to β -carotene as shown in the top of Table 4. The two basis sets of STO-3G and 6-31 G(d) were also implemented for the geometry optimized at HF/6-31G level to check the accuracy from starting cluster size of 6 units. The STO-3G results show around two-order improvement in the total energy by the new elongation method, while the 6-31G(d) results show around three-order improvement as seen in the case of polyacene. The errors caused by traditional elongation method become larger with basis sets size as seen from the table, while new treatment presented here is not so sensitive on the basis set used.

5.4 Lycopene

We applied the revised elongation method to another bio-system to confirm the applicability to yet another system.

As an example for a rather small but delocalized systems, our treatment was tested on the lycopene oligomer as shown in Table 5. Here we examined more details related to the B-region size dependency. The geometry was adopted from experimental data [47], but only hydrogens were optimized at the B3LYP/6-31G level. As for B-region = 3 units, the elongation started just after the starting cluster calculation of 5th (A-region = 2 and B-region = 3), since the definition of Eq. 3 to remove frozen orbitals was already smaller than the threshold at 5th units. The accuracy was drastically improved by four-orders of magnitude using the new elongation method. The N_{shift} denotes the number of frozen orbitals that were shifted to the active space. One can see that the number of the shifted orbitals is almost constant during the elongation. Therefore, the total number of active RLMOs does not accumulate with chain length even after the orbitals are shifted and thus the required CPU times at each step is almost kept constant during the elongation process. As for B-region = 4 units, the elongation started also just after the starting cluster calculation of 6th units, and the N_{shift} shows the same behavior as the case of B-region = 3 units. As for B-region = 5 units, similarly, the condition to remove frozen orbitals is satisfied in the starting cluster of 7th units. The errors caused by the new elongation method are almost the same $\sim 10^{-8-9}$ au/atom for all the three different B-region sizes. The N_{shift} coincided with one step later with increasing one B-region unit, because localization between A and B regions starts one step later. For example, $N_{\text{shift}} = 7$ for all different B-region sizes in the initial step means the number of shifted orbitals in the boundary 1st unit and 2nd unit just after starting cluster

Table 4 Error per atom (in au) introduced by the old and new elongation methods for β -carotene at the HF/STO-3G and 6-31G(d) level



Step	Number of units	Number of atoms	Old_Elg Error/atom	New_Elg Error/atom	Old_Elg Error /atom	New_Elg Error /atom
			STO-3G		6-31G(d)	
0	6	51	0.00E+00	0.00E+00	0.00E+00	0.00E+00
1	7	58	1.01E-07	7.43E-10	1.10E-06	3.31E-10
2	8	62	3.18E-07	8.94E-10	1.71E-06	1.60E-09
3	9	69	5.76E-07	1.88E-09	2.49E-06	1.42E-09
4	10	73	7.86E-07	2.90E-09	2.95E-06	2.47E-09
5	11	96	7.39E-07	6.07E-09	3.57E-06	2.47E-09

calculation toward 1st elongation step. But these orbitals are frozen in the next elongation step, and then 8 orbitals were newly selected for shifting to the active space in the second elongation step. Finally, we can conclude that the new elongation method detects automatically necessary orbitals to join the interaction with attacking monomer in “orbital basis concept” using Eq. 4 even if the B-region is small, and then we can start it with small starting cluster without loss of accuracy.

To confirm the reliability of our treatment for larger basis sets including diffuse and polarization functions, we perform the same calculation for lycopene using HF/6-31+G(d,p) basis set. From Table 6, one can see that the obtained total energy errors using large basis set are similar to the above results at 3-21G level or even more improved. Also we elongate it only with B region = 2 units, but elongation starts from end of 7th unit after the calculations using all the frozen and active LMOs for 4, 5 and 6 units because the condition Eq. 3 was not satisfied within the threshold until the 7th unit. This calculation with small B region size is actually the same as that using B region = 5 units. In principle, B region that is large enough to satisfy the required accuracy should be defined before starting elongation calculations. Nevertheless, in the new elongation method, the elongation is automatically initiated regardless of B region size, which always makes the task to define B region being easy even if starting B region = 1. These excellent results suggest no basis set dependency as

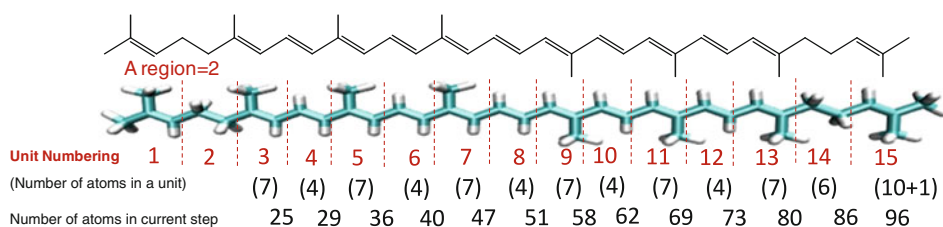
well as no B region size dependency on the accuracy of our new treatment.

5.5 Fullerene-polyacetylene- H_2 TPP

Next target of application is the examination of our treatment on some large intermolecular complexes through nano-wire of conducting oligomer. Recently, fullerene and porphyrin dyads of donor–acceptor (D-A) character are subjects of considerable interest because those two gigantic substitutions in the terminal are attracted to form host–guest complex. To understand the nature of the interaction between fullerene and chromophore dyads like porphyrin with different electron-donor character, several theoretical studies have been carried out for those complexes [48–51]. Here we adopted one of the most studied free base tetraphenylporphyrin (H_2 TPP) that constitutes an important class of π -conjugated organic chromophores and used to functionalize nanowires [52–56].

First, we applied our revised elongation method to the following $C_{60}-(C_4H_4)_n-H_2$ TPP system to see if this method is applicable or not to such gigantic delocalized systems. The calculations were performed by increasing the number of the (C_4H_4) units in the central wire part keeping terminated by C_{60} and H_2 TPP. The Table 7 shows that the accuracy is satisfied for such delocalized large systems also though it has lost around by one-order compared to that of other examples presented in aforementioned Sects. 5.1–5.4.

Table 5 Error per atom (in au) introduced by the old and new elongation methods for lycopene chain for different B region sizes at the HF/3-21G level



Number of units	Number of atoms	Old_Elg	New_Elg	N_{shift}	Old_Elg	New_Elg	N_{shift}	Old_Elg	New_Elg	N_{shift}
		Error/atom	Error/atom		Error/atom	Error/atom		Error/atom	Error/atom	
		B region=3 units			B region=4 units			B region=5 units		
5	36	0.00E+00	0.00E+00	7						
6	40	2.65E-05	-3.84E-09	8	0.00E+00	0.00E+00	7			
7	47	5.23E-05	2.16E-09	8	1.05E-06	-2.23E-10	8	0.00E+00	0.00E+00	7
8	51	6.75E-05	7.22E-09	7	3.38E-06	3.69E-10	8	1.58E-007	6.08E-011	8
9	58	8.69E-05	1.06E-08	8	4.77E-06	8.59E-10	7	4.96E-007	3.66E-010	8
10	62	9.17E-05	1.80E-08	8	6.78E-06	6.77E-09	8	8.36E-007	1.27E-009	7
11	69	1.09E-04	1.62E-08	8	8.41E-06	4.59E-09	8	1.18E-006	1.17E-009	8
12	73	1.18E-04	2.42E-08	10	1.04E-05	1.12E-08	8	1.50E-006	2.30E-009	8
13	80	1.20E-04	2.26E-08	7	1.08E-05	1.02E-08	10	1.69E-006	2.17E-009	8
14	86	1.27E-04	3.28E-08	10	1.11E-05	9.61E-09	7	1.77E-006	4.74E-009	10
15	96	1.14E-04	2.58E-08	-	9.88E-06	7.93E-09	-	1.60E-006	3.26E-009	-
		Sum of shifted orbitals		81	Sum of shifted orbitals		71	Sum of shifted orbitals		64

Table 6 Error per atom (in au) introduced by the new elongation method for lycopene chain with B region = 2 and 5 units at the HF/6-31 + G(d,p) level

Number of units	Number of atoms	New_Elg Error/atom	
		B region = 2 units	B region = 5 units
5	36	0.00E+00	
6	40	0.00E+00	
7	47	0.00E+00	0.00E+00
8	51	1.37E-11	9.22E-11
9	58	1.21E-10	1.09E-10
10	62	1.15E-10	1.23E-10

5.6 Fullerene–oligo(2,5-thienylene-ethynylene)–H₂TPP

Furthermore, we extend the system to a more realistic nanowire complex shown below in which the polyacetylene of above example was replaced by head-to-tail coupled polythiophene derivatives—[oligo(2,5-thienylene-ethynylene)]-(OTE)—terminated by the same fullerene and H₂TPP. The OTE wire part is a class of conjugated oligomers with a high shape-persistence as rigid rods and special attention is focused on the systems with terminal donor–acceptor substitution because of a strong push–pull effect [57–59].

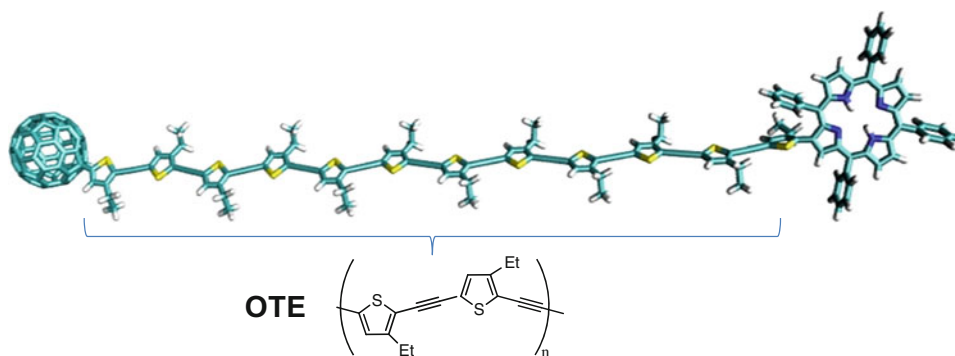
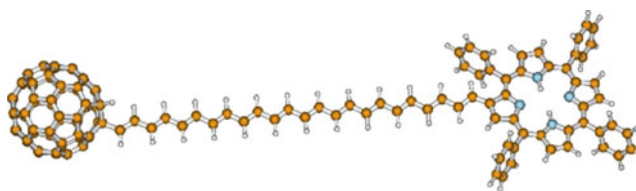


Table 7 Error per atom (in au) introduced by the new elongation method for C_{60} – $(C_4H_4)_n$ – H_2TPP system at the HF/3-21G level



Dyad	Number of atoms	Total energy Conv (in au)	Total energy Elg (in au)	ΔE (Elg-Conv)	New_Elg Error/atom
C_{60} – C_4H_4 – H_2TPP	146	-4302.7457358264	-4302.7457358232	3.17E-09	2.17E-11
C_{60} – $(C_4H_4)_2$ – H_2TPP	154	-4455.6587183241	-4455.6587162673	2.06E-06	1.34E-08
C_{60} – $(C_4H_4)_3$ – H_2TPP	162	-4608.5726760087	-4608.5726728645	3.14E-06	1.94E-08
C_{60} – $(C_4H_4)_4$ – H_2TPP	170	-4761.4867339248	-4761.4867312944	2.63E-06	1.55E-08
C_{60} – $(C_4H_4)_5$ – H_2TPP	178	-4914.4008358177	-4914.4007676444	6.82E-05	3.83E-07
C_{60} – $(C_4H_4)_6$ – H_2TPP	186	-5067.3149696281	-5067.3149674217	2.21E-06	1.19E-08

Polythiophenes have been extensively studied during last three decades. The pioneering works by Alan Heeger, Alan MacDiarmid, and Hideki Shirakawa in the field of conducting polymers gained international recognition by the awarding of the 2000 Nobel Prize in Chemistry “for the discovery and development of conductive polymers” [60–62]. These materials among other notable properties exhibit quite high electrical conductivity, which originates from the delocalization of electrons along the polymer backbone. Because of the extreme conductivity properties they are often regarded as “synthetic metals”. The electron delocalization gives rise also to optical phenomena. The optical properties of these materials respond to external perturbations, with significant color shifts in response to changes in solvent environment, temperature, applied potential, and binding to other molecules. The color and conductivity effects are governed by common mechanism which relies on twisting of the polymer backbone, disrupting conjugation. This makes conjugated polymers attractive for manufacturing sensors that can provide a wide range of optical and electronic responses. For this reason, the applicability of our method to such delocalized nanowires should be carefully checked for further applications of this method toward designing functional nanowire systems.

If our aim is only the final systems of the nanowire with terminal donor and acceptor, we can elongate either from C_{60} terminal of the wire and terminate with Porphyrin or from the central to the both end part as already performed for push–pull system [39]. Before calculation of the whole system, the accuracy of our treatment was investigated only for OTE wire part, and the errors obtained became improved by around three orders of magnitude in total energy/atom compared to those by the older conventional elongation method as shown in the Table 8, giving

extremely small errors $\sim 10^{-12}$ au/atom. So, we confirmed that the orbital shift treatment is a very useful method to get more accurate results for such π -electron delocalized systems. Additionally, as one of final purposes we calculated (hyper) polarizability of the OTE wire system and the obtained α , β , and γ values by the new elongation method and the conventional method were listed below the table for energy comparison. From very sensitive numerical instability in higher order derivatives by electronic field of total energy, the error in γ value becomes larger than α and β , but still is within $\sim 10^{-2}\%$ of the total value. These accuracies are very promising to investigate NLO properties even in such strongly delocalized systems. These NLO results from FF method depend only on the accuracy of the total energy for different fields, and thus, the obtained accuracies are reasonable as we already published NLO results for these field strengths (see for example, Refs. [37–42] for NLO results without the orbital shifted method). The NLO investigations for other systems are systematically ongoing and will be reported soon, though in the present article we just demonstrate one example to show how our new treatment is working for this property.

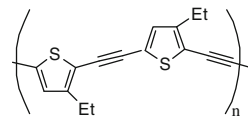
It is also very useful to see the wire’s effect under the influence of the big terminal substitutions. As another way to investigate the relationship between wire length and physical property, we can elongate the wire part—OTE—as the terminal substitution is fixed as shown in Table 9. We can elongate the chain with terminated H_2TPP molecules instead of hydrogen. This way for elongation, however, is time consuming as we have to keep the two big terminal molecules during elongation at least until AO-cut starts for removing C_{60} . Therefore, the right end of the chain was elongated with terminal hydrogen, and then H_2TPP was attached only at the final step, by which we can save computational time during elongation if we focus only

Table 8 (a) Error per atom (in au) introduced by the old and new elongation methods for OTE wire system at the HF/3-21G level and (b) Dipole Moment and (hyper)polarizability comparison at $n = 20$

(a)

Number of Unit*	Total energy Conv (in au)	Old_Elg Error/atom	New_Elg Error/atom
12	-8276.7158675228	6.00E-10	3.33E-12
14	-9668.4393841348	2.00E-10	9.53E-13
16	-11060.1629006892	1.30E-09	5.42E-12
18	-12451.8864172189	1.00E-09	3.71E-12
20	-13843.6253615705	1.40E-09	4.67E-12

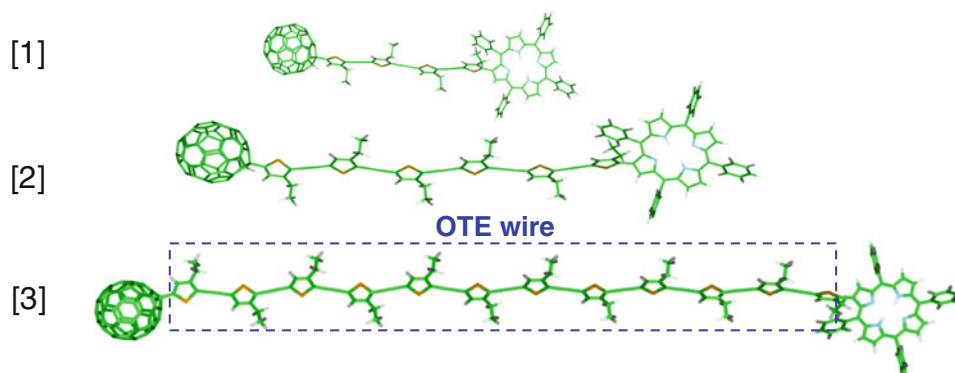
*Unit= two thiophene rings



(b)

Method	Dipole Moment & (Hyper)polarizability	Error (%)
New_Elg	μ_z (Debye)	1.648
Conv		6.68E-06
New_Elg	α_{zz} (au)	337.50
Conv		2.73E-05
New_Elg	γ_{zzzz} (au)	-1804
Conv		4.03E-01

Table 9 Error per atom (in au) introduced by the new elongation method for C_{60} -[OTE]- H_2 TPP system at the HF/3-21G level, where only final energies for [1], [2] and [3] were listed



Dyad	Number of atoms	Total energy Conv (in au)	Total energy Elg (in au)	$\Delta E(\text{Elg-Conv})$	New_Elg Error/atom
[1]	196	-6875.4797176171	-6875.479717505	1.12E-07	5.72E-10
[2]	226	-8275.9355460483	-8275.9355460401	8.20E-09	3.63E-11
[3]	316	-12477.3014981261	-12477.301498125	1.10E-09	3.48E-12

on the final C_{60} -[OTE]- H_2 TPP with different OTE lengths. The three models with different OTE lengths show the final structures after elongation. The calculated total energies show the excellent agreement with those by the direct calculations for whole system using the conventional direct method. These applications are promising enough to provide very reliable NLO property for gigantic systems that cannot be treated using the conventional direct method.

6 Concluding remarks

The elongation method has been further improved by orbital selection treatment to reconstruct necessary active RLMOs.

By this correction technique, a few initially defined frozen orbitals that are not well localized into frozen region are shifted to the active space. After testing it on SW-BN/C nanotube, polyacene, β -carotene, lycopene, fullerene- C_4H_4 - H_2 TPP, OTE, and fullerene-OTE- H_2 TPP, we have confirmed that the improved method becomes more applicable to strongly delocalized systems with high accuracy and with even more efficiency. This work now allows one to perform NLO property simulations for large systems with delocalization. In addition to applications, further development is ongoing to treat systems which require multireference ground-state wave functions, that is, RASSCF method and CASPT2 to treat dynamic correlation. We look forward in the near future to present new results in this area.

Acknowledgments One of the authors, O. L., acknowledges Japan Society for the Promotion of Science (JSPS) fellowship for financial support during stay at Kyushu University in Japan. This work was partly supported by a grant-in-aid from the Ministry of Education, Culture, Sports, Science and Technology (MEXT) of Japan and by the Asahi Glass Foundation. The calculations were carried out on the Linux cluster system in our laboratory and the high-performance computing system (Hitachi SR16000) of the Research Institute for Information Technology at Kyushu University. The authors are grateful to Prof. K. J. Jalkanen for careful English proofreading and editing of the manuscript.

References

1. Imamura A, Aoki Y, Maekawa K (1991) A theoretical synthesis of polymers by using uniform localization of molecular orbitals: Proposal of an elongation method. *J Chem Phys* 95:5419–5431
2. Aoki Y, Imamura A (1992) Local density of states of aperiodic polymers using the localized orbitals from an ab initio elongation method. *J Chem Phys* 97:8432–8440
3. Aoki Y, Suhai S, Imamura A (1994) An efficient cluster elongation method in density functional theory and its application to polyhydrogen-bonding molecules. *J Chem Phys* 101:10808–10823
4. Makowski M, Korchowiec J, Gu FL, Aoki Y (2010) Describing electron correlation effects in the framework of the elongation method—Elongation-MP2: formalism, implementation and efficiency. *J Comput Chem* 31:1733–1740
5. Gu FL, Imamura A, Aoki Y (2006) Elongation method for polymers and its application to nonlinear optics, in atoms, molecules and clusters in electric fields: theoretical approaches to the calculation of electric polarizabilities. In: Maroulis G (ed) *Computational numerical and mathematical methods in sciences and engineering*, Imperial College Press, London, 1:97–177. <http://www.icpress.co.uk/chemistry/p464.html>
6. Goedecker S (1999) Linear scaling electronic structure methods. *Rev Mod Phys* 71:1085–1123
7. Salek P, Hoest S, Thoegersen L, Joergensen P, Manninen P, Olsen J, Jansik B, Reine S, Pawlowski F, Tellgren E, Helgaker T, Coriani S (2007) Linear-scaling implementation of molecular electronic self-consistent field theory. *J Chem Phys* 126:114110
8. Goedecker S, Teter M (1995) Tight-binding electronic-structure calculations and tight-binding molecular dynamics with localized orbitals. *Phys Rev B* 51:9455–9464
9. Stephan U, Drabold D (1998) Order-N projection method for first-principles computations of electronic quantities and Wannier functions. *Phys Rev B* 57:6391–6407
10. Li X-P, Nunes W, Vanderbilt D (1993) Density-matrix electronic-structure method with linear system-size scaling. *Phys Rev B* 47:10891–10894
11. Zhao Q, Yang W (1995) Analytical energy gradients and geometry optimization in the divide-and-conquer method for large molecules. *J Chem Phys* 102:9598–9603
12. Kim J, Mauri F, Galli G (1995) Total-energy global optimizations using nonorthogonal localized orbitals. *Phys Rev B* 52:1640–1648
13. Hernandez E, Gillan M (1995) Self-consistent first-principles technique with linear scaling. *Phys Rev B* 51:10157–10160
14. Yang W (1991) Direct calculation of electron density in density-functional theory. *Phys Rev Lett* 66:1438–1441
15. Yang W, Lee T-S (1995) A density-matrix divide-and-conquer approach for electronic structure calculations of large molecules. *J Chem Phys* 103:5674–5678
16. Akama T, Kobayashi M, Nakai H (2007) Implementation of divide-and-conquer method including Hartree-Fock exchange interaction. *J Comput Chem* 28:2003–2012
17. Kobayashi M, Imamura Y, Nakai H (2007) Alternative linear-scaling methodology for the second-order Møller-Plesset perturbation calculation based on the divide-and-conquer method. *J Chem Phys* 127:074103
18. Kitaura K, Ikeo E, Asada T, Nakano T, Uebayasi M (1999) Fragment molecular orbital method: an approximate computational method for large molecules. *Chem Phys Lett* 313:701–706
19. Fedorov DG, Kitaura K (2004) The importance of three-body terms in the fragment molecular orbital method. *J Chem Phys* 120:6832–6840
20. Fedorov DG, Kitaura K (2004) On the accuracy of the 3-body fragment molecular orbital method (FMO) applied to density functional theory. *Chem Phys Lett* 389:129–134
21. Fedorov DG, Kitaura K (2007) Extending the power of quantum chemistry to large systems with the fragment molecular orbital method. *J Phys Chem A* 111:6904–6914
22. Mochizuki Y, Koikegami S, Nakano T, Amari S, Kitaura K (2004) Large scale MP2 calculations with fragment molecular orbital scheme. *Chem Phys Lett* 396:473–479
23. Mochizuki Y, Fukuzawa K, Kato A, Tanaka S, Kitaura K, Nakano T (2005) A configuration analysis for fragment interaction. *Chem Phys Lett* 410:247–253
24. Mochizuki Y, Ishikawa T, Tanaka K, Tokiwa H, Nakano T, Tanaka S (2006) Dynamic polarizability calculation with fragment molecular orbital scheme. *Chem Phys Lett* 418:418–422
25. Mochizuki Y, Yamashita K, Murase T, Nakano T, Fukuzawa K, Takematsu K, Watanabe H, Tanaka S (2008) Large scale FMO-MP2 calculations on a massively parallel-vector computer. *Chem Phys Lett* 457:396–403
26. White SR (1992) Density matrix formulation for quantum renormalization groups. *Phys Rev Lett* 69:2863–2866
27. Kurashige Y, Yanai T (2009) High-performance ab initio density matrix renormalization group method: applicability to large-scale multireference problems for metal compounds. *J Chem Phys* 130:234114
28. Mizukami W, Kurashige Y, Yanai T (2010) Communication: novel quantum states of electron spins in polycarbenes from ab initio density matrix renormalization group calculations. *J Chem Phys* 133:091101
29. Gu FL, Aoki Y, Korchowiec J, Imamura A, Kirtman B (2004) A new localization scheme for the elongation method. *J Chem Phys* 121:10385–10391
30. Aoki Y, Gu FL (2009) Generalized elongation method: from one-dimension to three-dimension. In Champagne B, Gu FL, Luis JM, Springborg M (org) *International conference of computational methods in sciences and engineering 2009 (ICCMSE 2009)* 46–49. <http://www.uni-saarland.de/fak8/springborg/ICCMSE2009/boax.pdf>
31. Makowski M, Gu FL, Aoki Y (2010) Elongation-CIS method: describing excited states of large molecular systems in regionally localized molecular orbital basis. *J Comput Method Sci Eng* 10:473–481. doi:10.3233/JCM-2010-0312. <http://iospress.metapress.com/content/7c71004j74717106/fulltext.pdf>
32. Korchowiec J, Gu FL, Imamura A, Kirtman B, Aoki Y (2005) Elongation method with cutoff technique for linear SCF scaling. *Int J Quantum Chem* 102:785–794
33. Makowski M, Korchowiec J, Gu FL, Aoki Y (2006) Efficiency and accuracy of the elongation method as applied to the electronic structures of large systems. *J Comp Chem* 27:1603–1619
34. Korchowiec J, Lewandowski J, Makowski M, Gu FL, Aoki Y (2009) Elongation cutoff technique armed with quantum fast multipole method for linear scaling. *J Comput Chem* 30:2515–2525
35. Korchowiec J, Silva P, Makowski M, Gu FL, Aoki Y (2010) Elongation cutoff technique at Kohn–Sham level of theory. *Int J Quantum Chem* 110:2130–2139

36. Gu FL, Aoki Y, Imamura A, Bishop DM, Kirtman B (2003) Application of the elongation method to nonlinear optical properties: finite field approach for calculating static electric (hyper)polarizabilities. *Mol Phys* 101:1487–1494
37. Ohnishi S, Gu FL, Naka K, Imamura A, Kirtman B, Aoki Y (2004) Calculation of static (Hyper) polarizabilities for π -conjugated donor/acceptor molecules and block copolymers by the elongation finite-field method. *J Phys Chem A* 108:8478–8484
38. Gu FL, Guillaume M, Botek E, Champagne B, Castet F, Ducasse L, Aoki Y (2006) Elongation method and supermolecule approach for the calculation of nonlinear susceptibilities. Application to the 3-methyl-4-nitropyridine 1-oxide and 2-methyl-4-nitroaniline crystals. *J Comput Method Sci Eng* 6:171–188. <http://iospress.metapress.com/content/fwabp9hpr2nr7mhh/fulltext.pdf>
39. Ohnishi S, Orimoto Y, Gu FL, Aoki Y (2007) Nonlinear optical properties of polydiacetylene with donor-acceptor substitution block. *J Chem Phys* 127:084702
40. Chen W, Yu G-T, Gu FL, Aoki Y (2009) Investigation on the electronic structures and nonlinear optical properties of pristine boron nitride and boron nitride-carbon heterostructured single-wall nanotubes by the elongation method. *J Phys Chem C* 113:8447–8454
41. Yan LK, Pomogaeva A, Gu FL, Aoki Y (2010) Theoretical study on nonlinear optical properties of metalloporphyrin using elongation method. *Theor Chem Acc* 125:511–520
42. Pomogaeva A, Gu FL, Imamura A, Aoki Y (2010) Electronic structures and nonlinear optical properties of supramolecular associations of benzo-2, 1, 3-chalcogendiazoles by the elongation method. *Theor Chem Acc* 125:453–460
43. Schmidt MW, Baldrige KK, Boatz JA, Elbert ST, Gordon MS, Jensen JH, Koseki S, Matsunaga N, Nguyen KA, Su SJ, Windus TL, Dupuis M, Montgomery JA (1993) General atomic and molecular electronic structure system. *J Comput Chem* 14:1347–1363. <http://www.msg.ameslab.gov/gamess/index.html>
44. Blase X, Charlier JC, De Vita A, Car R (1999) Structural and electronic properties of composite BxCyNz nanotubes and heterojunctions. *Appl Phys A* 68:293–300
45. Terrones M, Romo-Herrera JM, Cruz-Silva E, Lopez-Urias F, Munoz-Sandoval E, Velazquez-Salazar JJ, Terrones H, Bando Y, Golberg D (2007) Pure and doped boron nitride nanotubes. *Mater Today* 10:30–38
46. Frisch MJ, Trucks GW, Schlegel HB, Scuseria GE, Robb MA, Cheeseman JR, Montgomery JA Jr, Vreven T, Kudin KN, Burant JC, Millam JM, Iyengar SS, Tomasi J, Barone V, Mennucci B, Cossi M, Scalmani G, Rega N, Petersson GA, Nakatsuji H, Hada M, Ehara M, Toyota K, Fukuda R, Hasegawa J, Ishida M, Nakajima T, Honda Y, Kitao O, Nakai H, Klene Li X, Knox JE, Hratchian HP, Cross JB, Adamo C, Jaramillo J, Gomperts R, Stratmann RE, Yazyev O, Austin AJ, Cammi R, Pomelli C, Ochterski JW, Ayala PY, Morokuma K, Voth GA, Salvador P, Dannenberg JJ, Zakrzewski VG, Dapprich S, Daniels AD, Strain MC, Farkas O, Malick DK, Rabuck AD, Raghavachari K, Foresman JB, Ortiz JV, Cui Q, Baboul AG, Clifford S, Cioslowski J, Stefanov BB, Liu G, Liashenko A, Piskorz P, Komaromi I, Martin RL, Fox DJ, Keith T, Al-Laham MA, Peng CY, Nanayakkara A, Challacombe M, Gill PMW, Johnson B, Chen W, Wong MW, Gonzalez C, Pople JA (2004) Gaussian 03, Revision C.02. Gaussian, Inc., Wallingford, CT
47. <http://xray.bmc.uu.se/hicup/LYC/index.html#COO>
48. Liao M-S, Watts JD, Huang M-J (2009) Dispersion-corrected DFT calculations on C60-porphyrin complexes. *Phys Chem Chem Phys* 11:4365–4374
49. Loboda O, Zalesny R, Avramopoulos A, Papadopoulos MG, Artacho E (2009) Linear—scaling calculations of linear and nonlinear optical properties of [60]fullerene derivatives. In Maroulis G, Simos TE (ed) *Computational methods in sciences and engineering, advances in computational science book series: AIP conference proceedings* 1108:198–204. <http://link.aip.org/link/APCPCS/1108/198/1>
50. Loboda O, Zalesny Avramopoulos A, Luis J-M, Kirtman B, Tagmatarchis N, Reis H, Papadopoulos MG (2009) Linear and nonlinear optical properties of [60]fullerene derivatives. *J Phys Chem A* 113:1159–1170
51. Zalesny R, Loboda O, Iliopoulos K, Chatzikyriakos G, Couris S, Rotas G, Tagmatarchis N, Avramopoulou A, Papadopoulos MG (2010) Linear and nonlinear optical properties of triphenylamine-functionalized C60: insights from theory and experiment. *Phys Chem Chem Phys* 12:373–381
52. Palumbo M, Hogan C, Sottile F, Bagalá P, Rubio A (2009) Ab initio electronic and optical spectra of free-base porphyrins: the role of electronic correlation. *J Chem Phys* 131:084102
53. Yeon KY, Jeong D, Kim SK (2010) Intrinsic lifetimes of the Soret bands of the free-base tetraphenylporphine (H2TPP) and Cu(II)TPP in the condensed phase. *Chem Commun* 46:5572–5574
54. Li C, Ly J, Lei B, Fan W, Zhang D, Han J, Mayyappan M, Thompson C, Zhou M (2004) Data storage studies on nanowire transistors with self-assembled porphyrin molecules. *J Phys Chem B* 108:9646–9649
55. Kwok KS (2003) Materials for future electronics. *Mater Today* 6:20–27
56. Duan X, Huang Y, Lieber CM (2002) Nonvolatile memory and programmable logic from molecule-gated nanowires. *Nano Lett* 2:487–490
57. Meier H, Mühling B (2009) Synthesis and properties of oligo (2,5-thienylene)s. In Waring A (ed) *ARKIVOC: Special issue '5th Eurasian conference on heterocyclic chemistry'* ix: 57–69. <http://www.arkat-usa.org/get-file/25267/>
58. Obara Y, Takimiya K, Aso Y, Otsubo T (2001) Synthesis and photophysical properties of [60]fullerene-oligo(thienylene-ethynylene) dyads. *Tetrahedron Lett* 42:6877–6881
59. Tormos GV, Nugara PN, Lakshminantham MV, Gava MP (1993) Poly(2,5-thienylene ethynylene) and related oligomers. *Synth Met* 53:271–281
60. Shirakawa H, Louis EJ, MacDiarmid AG, Chiang CK., Heeger AJ (1977) Synthesis of electrically conducting organic polymers: halogen derivatives of polyacetylene, (CH)_x. *J Chem Soc Chem Commun* 1977:578–580
61. Chiang CK, Druy MA, Gau SC, Heeger AJ, Louis EJ, MacDiarmid AG, Park YW, Shirakawa H (1978) Synthesis of highly conducting films of derivatives of polyacetylene, (CH)_x. *J Am Chem Soc* 100:1013–1015
62. MacDiarmid AG (2001) Synthetic metals: a novel role for organic polymers. *Synth Met* 125:11–22